

Solar Salt Doped with Nano Additive Expanded Graphite as a Promising Phase Change Material for Thermal Energy Storage Systems

Priyanka¹, N Shanmuga priya²

^{1,2}Department of Mechanical Engineering, Siddaganga Institute of Technology (Autonomous Institution Affiliated to Visvesvaraya Technological University, Belagavi), Tumakuru 572 103, Karnataka, India.

Received 29 Oct 2024

Accepted 12 Jan 2025

Abstract

In solar thermal power generation plants, solar salt (a combination of KNO_3 and NaNO_3) is utilized as a thermal storage medium, thanks to its optimal phase change temperature, high heat storage density, and cost-effectiveness. The applications of few organic and inorganic storage materials are found to be limited, due to its low thermal conductivity during heat absorption and release process. Expanded graphite (EG) can be used as an additive to compensate for the solar salt's low thermal conductivity. The ultrasonic smashing method was used to prepare the binary nitrate in the weight ratio of 6:4 for $\text{NaNO}_3:\text{KNO}_3$. In this study, EG with weight percentage of 3%, 5%, 7%, and 9% were used to improve the thermal conductivity of solar salt. Thermal behaviors of the prepared sample were investigated with the help of differential scanning calorimeter (DSC). Scanning electron microscope (SEM) with EDX and X-ray diffraction (XRD) were utilized to characterize the morphology and chemical composition of pure EG, nitrate/EG composite phase change materials (PCM's) and binary nitrates. FT-IR spectroscopy is used to confirm the composite formation. In order to determine the thermal conductivity hot disk method was used. The binary nitrates/EG composite materials have been discovered to promise the reliable PCM for high temperature solar energy storage applications.

© 2025 Jordan Journal of Mechanical and Industrial Engineering. All rights reserved

Keywords: Expanded graphite, Phase change materials, Thermal energy storage.

1. Introduction

The growing global energy demand, driven by climate change, diminishing fossil fuel reserves, rising greenhouse gas emissions, and increasing fuel prices, has accelerated the shift toward renewable energy sources. Solar, wind, tidal, and geothermal energy are among the most promising solutions for meeting energy needs sustainably. Of these, solar energy is widely favored for its abundance and ease of access. However, the primary drawback of renewable energy sources, including solar energy, is their intermittent availability [M. Al Zou'bi 2010]. Solar energy, for instance, is unavailable during nighttime, necessitating the use of energy storage systems like Thermal Energy Storage (TES) to store excess energy during periods of availability and release it as needed.

TES systems have gained significant attention due to their ability to balance energy supply and demand, ensuring consistent energy availability. They play a crucial role in reducing dependency on alternative generators, optimizing energy distribution during peak periods, and minimizing environmental impact [A. Lazaro et al. (2009), A.A. Al-Abidi et al. (2012)]. TES technology stores

thermal energy in the form of heat or cold, using processes such as heating, cooling, and phase changes. Among the three types of TES systems—sensible heat, latent heat, and chemical storage—latent heat storage (LHS) stands out for its superior energy density and isothermal operation during phase transitions [K. Kant et al.(2016)].

LHS systems store energy by utilizing the heat absorbed or released during phase changes without significant temperature variation. They are more efficient than sensible heat systems, as demonstrated in various applications. For example, Bal et al. (2011) highlighted their potential in agricultural applications, while Huang et al. (2006) and Salem Nijmeh et al. (2020) demonstrated their effectiveness in mitigating temperature rise in building-integrated photovoltaics. Similarly, Biwole et al. (2013) discussed the benefits of LHS in improving solar panel performance [R. Pasupathy et al.(2008)].

LHS systems are widely utilized due to their high energy storage capacity and adaptability. Shalaby et al. (2014) and Mohamad et al. (2021) explored their application in solar dryers using phase change materials (PCM), while Sharma et al. (2009) reviewed their use in diverse thermal energy storage applications. Tyagi et al. (2007) emphasized their role in building thermal

* Corresponding author e-mail: nspriya@sit.ac.in.

management, and Waqas et al. (2013) highlighted their effectiveness in providing free cooling for buildings.

In concentrated solar power (CSP) applications, TES systems are essential for improving efficiency and reliability [Maher M et.al, 2017]. Solar salt, a eutectic mixture of sodium nitrate (NaNO_3) and potassium nitrate (KNO_3), is a widely used storage material due to its thermal stability, affordability, and availability. However, its low thermal conductivity presents a challenge for efficient heat transfer [Yang et al., 2018].

To address this limitation, researchers have incorporated expanded graphite (EG) into solar salt, significantly enhancing its thermal conductivity. Yang et al. (2018) demonstrated a 3–4-fold increase in thermal conductivity through EG doping, while Zhou et al. (2020) showed that EG improved thermal cycling efficiency and reduced melting and freezing times. Hybrid composites combining solar salt, EG, and carbon nanotubes further enhance thermal conductivity and latent heat storage capacity, offering a dual benefit for high-efficiency TES systems [Chen et al., 2017].

Recent studies have confirmed the long-term stability of solar salt/EG composites. Li et al. (2022) demonstrated consistent thermal performance over 300 cycles with 3 wt% EG, while Sun et al. (2016) reported improved thermal conductivity in a 5 wt% EG composite. These findings highlight the durability and effectiveness of EG-doped solar salt composites for practical applications.

In CSP systems and high-temperature heat exchangers, EG-doped solar salt composites have proven to reduce thermal losses and enhance system efficiency [Hassan Hadi et.al, 2022]. Teng et al. (2020) demonstrated their application in CSP systems, achieving better heat transfer and storage efficiency, while Gao et al. (2023) highlighted their role in minimizing thermal losses in high-temperature applications.

These advancements underscore the potential of solar salt/EG composites as a solution to the limitations of conventional TES materials, paving the way for more efficient and sustainable CSP technologies.

2. EXPERIMENT

2.1. Materials Selection and Preparation

The PCM selection process considers multiple factors, including its application in Latent Heat Storage (LHS). Researchers delve into the kinetic, thermodynamic, chemical, and economic aspects of PCM design. Numerous studies have investigated PCMs for LHS, examining their thermal, physical, kinetic, chemical, and cost-effective attributes. Thermal properties are crucial, encompassing the phase-transition temperature's appropriateness and a high latent heat across both phases' melting and solidification processes. The PCM's phase change temperature must align with the working temperature of the application. Higher latent heat per volume aids in reducing storage container size and PCM quantity. Meanwhile, elevated specific heat and thermal conductivity facilitate more efficient Sensible Heat Storage (SHS) and shorter phase transition times, ensuring consistent temperature distribution within the storage unit. Our material selection was guided by the established

temperature range for our experimental work. In this context, the eutectic mixture of NaNO_3 and KNO_3 (60:40), known as solar salt, proved optimal for temperatures exceeding 200°C . Table 1 outlines the properties of this eutectic salt.

Table 1. The properties of base PCM

Material	Melting point($^\circ\text{C}$)	Latent Heat(J/kg)	Specific heat (kJ/kgK)	Density (kg/m^3)	Thermal conductivity (W/m-K)
$\text{NaNO}_3/\text{KNO}_3$ (60:40)	223.2	92.32	2.351	1899	0.5
NaNO_3	308	157.14	0.465	7833	0.853
KNO_3	334	79.11	0.632	2110	0.531

Initially, powdered sodium nitrate and potassium nitrate were uniformly mixed. The EG were then added to nitrate mixture in mass fractions of 3%, 5 %, 7 %, or 9 %. The samples were prepared in two steps. The nanoparticles were mixed with molten salt and distilled water (150 ml), followed by a 200-minute sonication process to ensure good nanoparticle dispersion within the sample. The water in the samples was then completely evaporated in a muffle furnace at around 250°C .

2.2. Characterization Techniques

The characterization of nanoparticle-dispersed PCMs is crucial for enhancing heat transfer and evaluating material quality [K. V. Gangadharan et al. 2011 and Malek Ali et al. 2014]. It involves analyzing the size, shape, crystalline structure, chemical stability, phase change temperatures, latent heats, thermal conductivity, and thermal stability.

SEM (JEOL JCM 6000Plus) imaging examines nanoparticle dispersion and morphology in PCMs by utilizing a focused electron beam instead of light. This microscope's electron gun emits a beam that interacts with the sample, generating secondary electrons collected by detectors to create an image displayed on a computer screen. A field emission cathode in the electron gun produces a finely focused beam with variable electron energy, minimizing sample damage and charging while improving spatial resolution. EDX analysis, occasionally attached to SEM, detects elemental composition in nanoparticles.

XRD (Rigaku Ultima III) with Cu K-alpha radiation investigates crystal size and stability of pure molten salt samples with varying percentages of EG. XRD results assess crystallite structure and stability with and without different EG percentages.

FT-IR spectrometers (Shimadzu) measure spectra from 4000 cm^{-1} to 400 cm^{-1} . In this study, samples mixed with KBr crystal are pressed into tablet form to investigate specific interactions between NPs and base PCM.

DSC (Differential Scanning Calorimetry) determines heat capacity by measuring heat flow differences between sample and reference pans at the same temperature. Peaks in DSC curves indicate phase transitions, such as melting or freezing, revealing phase transition temperatures and latent heats. Using a Perkin Elmer DSC 2008 instrument with a heating rate of 5°C and nitrogen as a cooling medium, latent heats and phase change temperatures of base and Nano PCMs are determined.

3. RESULTS AND DISCUSSION

3.1. NDPCM Surface Morphology

The SEM analysis explored the microstructure and morphology of molten salt samples containing 3%, 5%, 7%, and 9% EG. Figure 2 (a) displays SEM images at

500µm magnification of pure NaNO₃, KNO₃, and EG, while Figure 2 (b) exhibits images at 50µm magnification showcasing molten salt samples with varying weight fractions of EG. Across all weight fractions, the SEM images consistently demonstrate the uniform distribution of the Nano additive EG within the NaNO₃/KNO₃ base material.

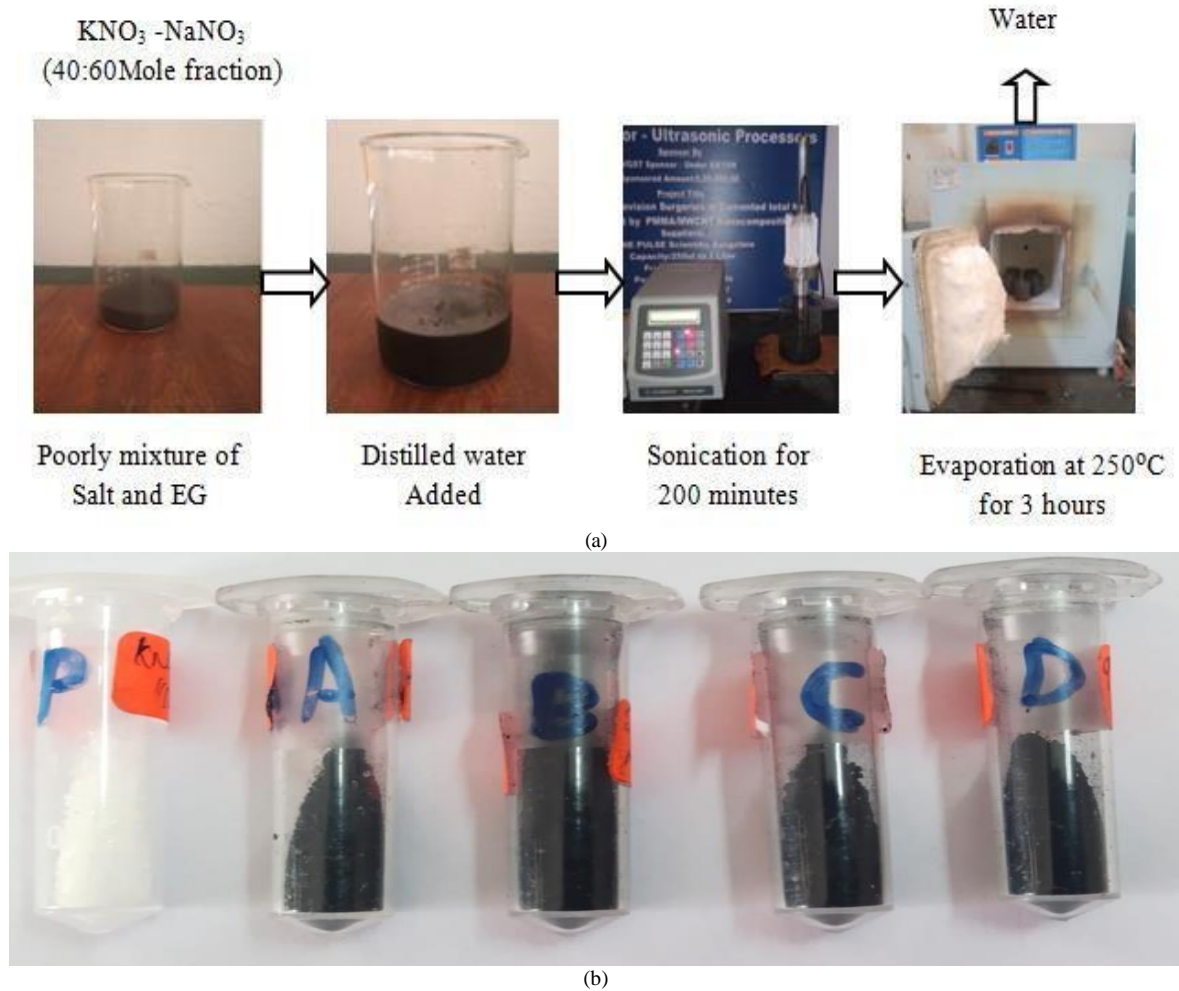


Figure 1. (a) Two-step synthesis of NDPCM and (b) Prepared specimen –sample P (Molten salt), sample A (3% NP), sample B (5% NP), sample C (7% NP) and sample D (9% NP)

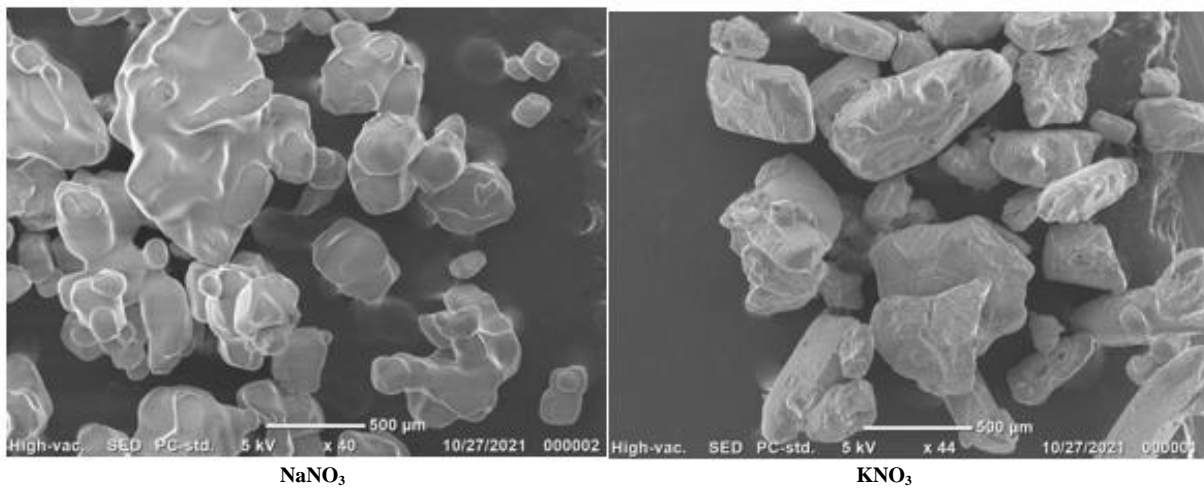


Figure 2. (a) SEM image of NaNO₃ and KNO₃ at magnification of 500µm

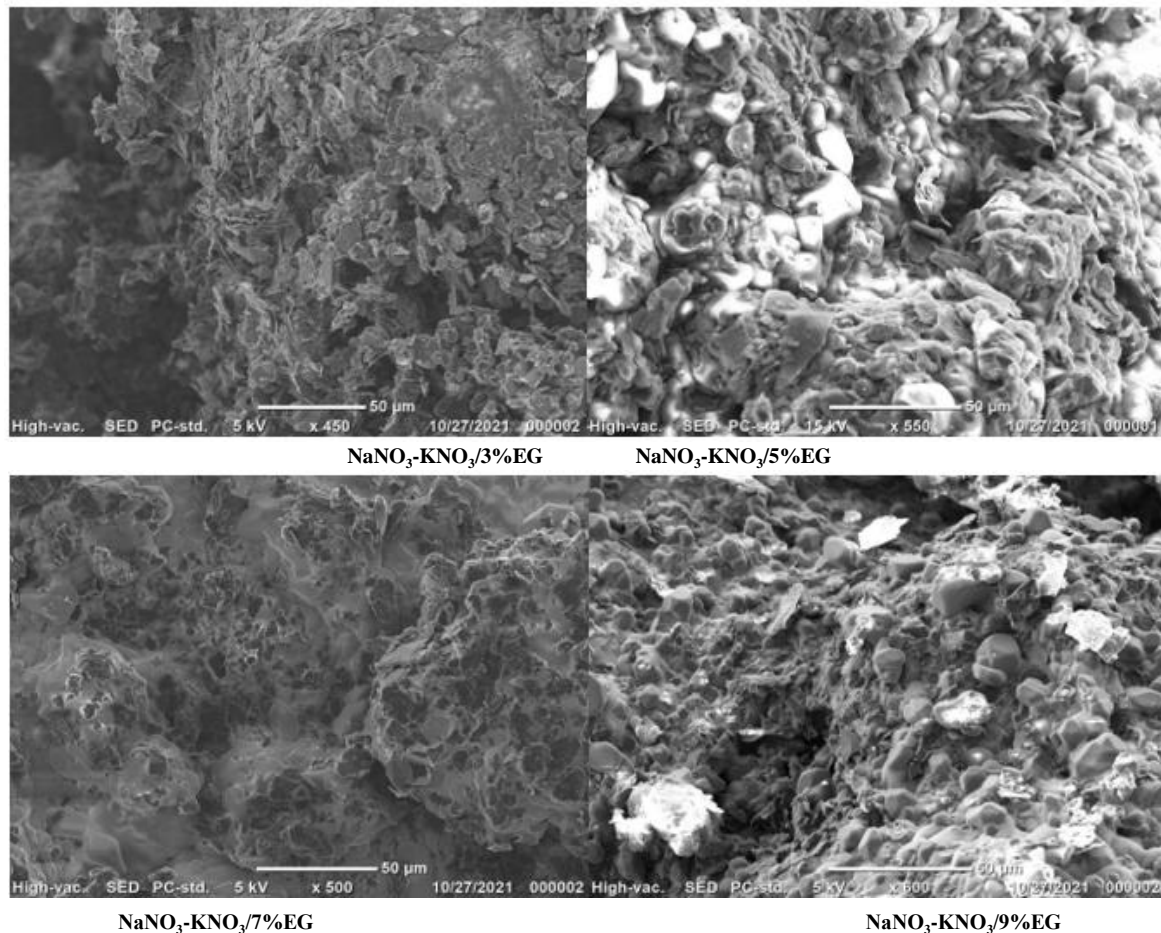


Figure 2. (b) SEM image of NaNO_3 , KNO_3 and different concentration of EG at magnification of $50\mu\text{m}$

3.2. EDX Analysis

Figures 3 (a) and 3 (b) show the EDX of molten salts with EG. Elementary composition of the prepared composites were observed and identified by EDX. The energy level peaks in EDX spectrum are observed to be distinctive to an atom which corresponds to a single element. The intensity peak in the EDX spectrum indicates that elements in specimen are more concentrated. Here high peak indicates a higher carbon concentration, when compared to the EDX of KNO_3 and NaNO_3 . The high intensity peak observed in KNO_3 was due to higher crystal agglomeration and its particle size.

3.3. X-Ray Diffraction Analysis

The XRD pattern of pure $\text{KNO}_3:\text{NaNO}_3(60:40)$ and $\text{KNO}_3:\text{NaNO}_3(60:40)$ with 3%, 5%, 7% and 9% EG are

shown in Figure 4. The scattering angle covered was from 0° to 90° . The diffraction peaks were observed at $18.85, 23.45, 29.36, 33.82, 42.03$ and 54.36 . For the $\text{KNO}_3:\text{NaNO}_3(60:40)$. For $\text{KNO}_3:\text{NaNO}_3$ with 3% EG, the peaks were observed at $23.77, 26.25, 28.38, 33.97, 41.04$, and 54.52 . For $\text{KNO}_3:\text{NaNO}_3$ with 5% EG, the peaks were observed at $23.45, 26.41, 31.18, 33.64, 40.87$ and 54.20 . For $\text{KNO}_3:\text{NaNO}_3$ with 7% EG, the peaks were observed at $23.45, 26.74, 29.54, 32.81, 33.82, 41.20$ and 44.33 . For $\text{KNO}_3:\text{NaNO}_3$ with 9% EG, the peaks were observed at $23.45, 26.41, 29.36, 32.16, 34.31, 41.04$ and 54.52 . The higher diffraction peaks were observed at $28.38, 31.3, 32.81$ and 34.31 for 3%, 5%, 7% and 9%, respectively. When EG was added to NDPCM, peaks with intensities similar to $\text{KNO}_3:\text{NaNO}_3(60:40)$ appeared, proving that EG had no impact on the molten salt's crystal structure.

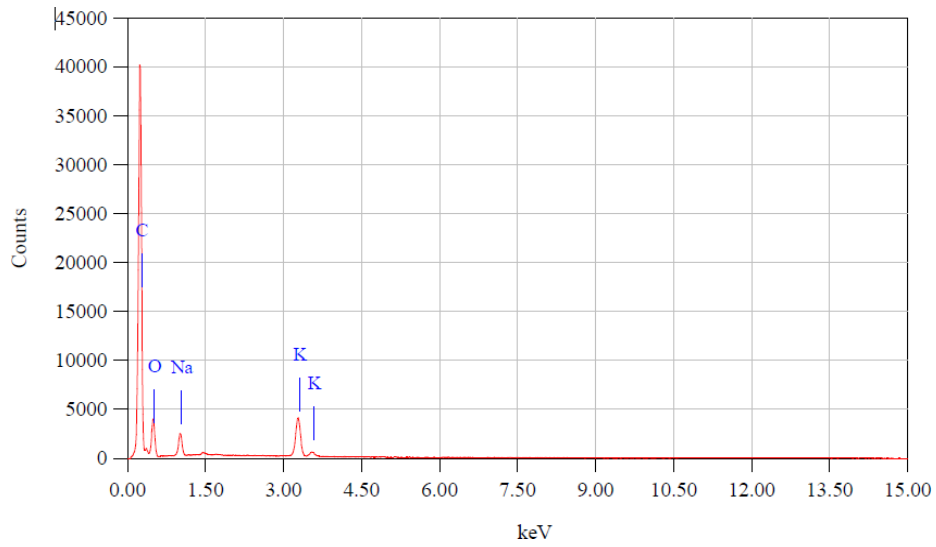


Figure 3. (a) EDX of $\text{KNO}_3:\text{NaNO}_3(60:40)/\text{EG}(3\%)$

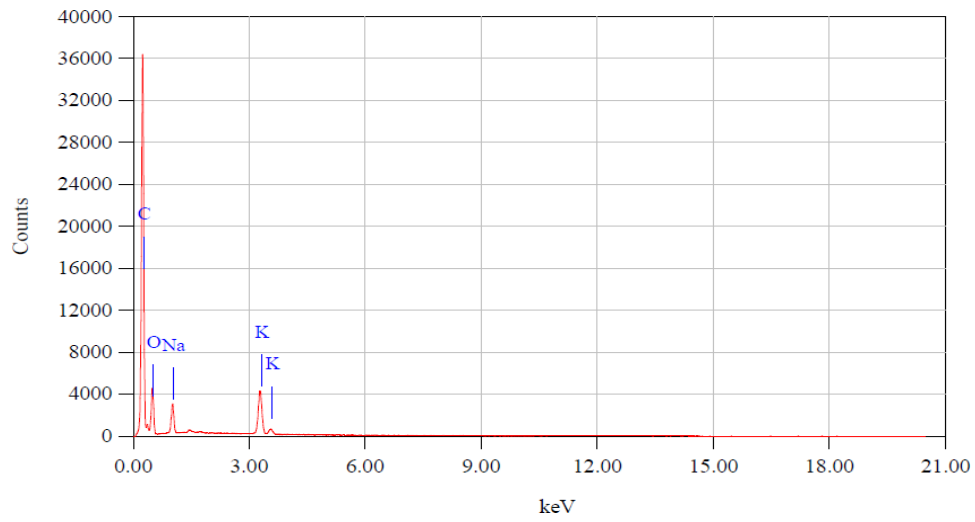


Figure 3. (b) EDX of $\text{KNO}_3:\text{NaNO}_3(60:40)/\text{EG}(9\%)$

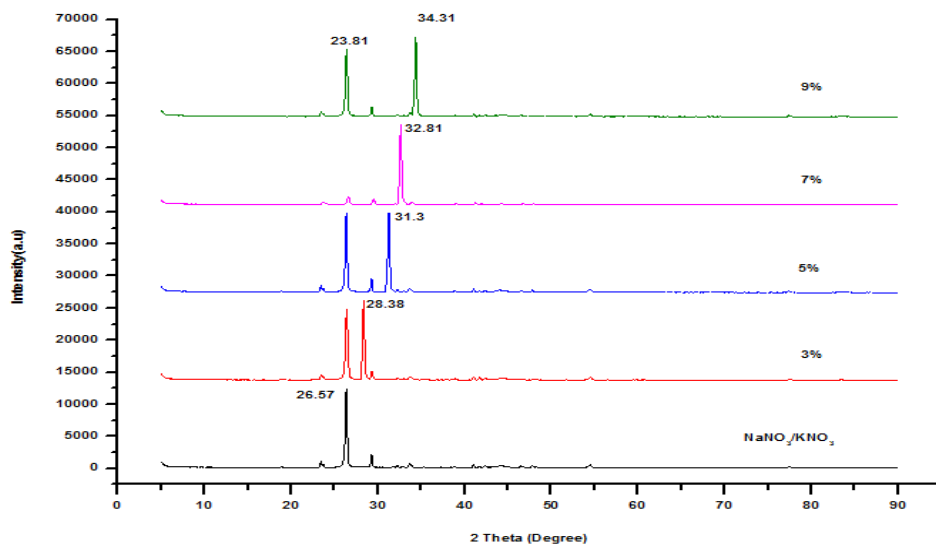


Figure 4. XRD pattern of $\text{NaNO}_3/\text{KNO}_3$ and $\text{NaNO}_3/\text{KNO}_3$ with different weight %EG

3.4. Fourier Transform Infrared Spectroscopy

FTIR spectra of molten salt with different EG nanomaterial are shown in Figure 5. FTIR is used to reveals the specific interaction bonds in PCM embedded with nanomaterial. The characteristics peaks from 400-4000 cm^{-1} confirms the incorporation of PCM with EG. In graph the characteristics like 3645, 3019, 1538, 1219, 1143, 993, 911, 799 cm^{-1} proves the existence $\text{KNO}_3/\text{NaNO}_3$ with EG. The peaks difference between pure molten salt and EG added molten salt is negligible. The absence of chemical reaction between the molten salt and EG was ensured from these FTIR spectra.

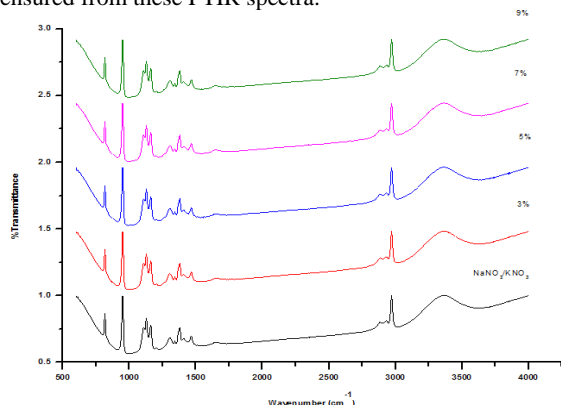


Figure 5. FT-IR spectra for $\text{KNO}_3/\text{NaNO}_3$ with different weight% EG

3.5. Differential Scanning Calorimeter

Figure 6 displays the DSC curves for the PCM/EG compositions at 3%, 5%, 7%, and 9%. All curves contain two phase transitions, one roughly at around 130°C and the other at around 223°C. In DSC results, two distinct exothermic peaks were identified during the heating process. The melting peak temperatures of the prepared samples was increased by to 0.16°C (3% EG), 0.31°C (5% EG), 0.46°C (7% EG) and 1°C (9% EG) compared with pure $\text{KNO}_3/\text{NaNO}_3$.

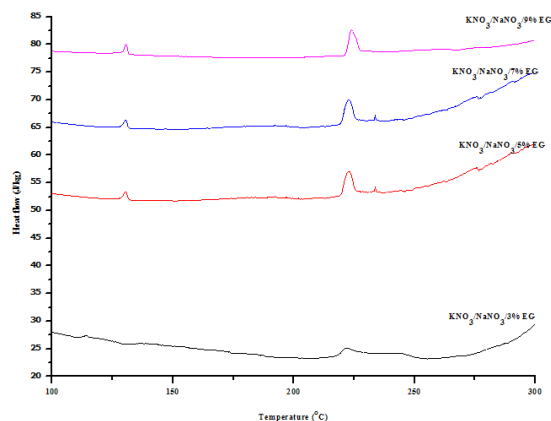


Figure 6. DSC curves for $\text{KNO}_3/\text{NaNO}_3$ with different EG mass fractions.

The observed increase in melting peak temperatures of $\text{KNO}_3/\text{NaNO}_3$ samples with expanded graphite (EG) can be attributed to the interaction between the molten salts and the EG matrix. When molten salts are incorporated into the porous structure of EG, the confinement can alter their thermophysical properties, including melting behavior. This phenomenon, known as the "confinement effect," can lead to an elevation in melting temperatures due to restricted molecular mobility within the confined spaces.

Additionally, the high thermal conductivity of EG facilitates more efficient heat distribution throughout the composite material. This enhanced heat transfer can influence the melting process, potentially causing a shift in the observed melting peak temperatures. A study on $\text{NaNO}_3\text{-KNO}_3/\text{EG}$ composites reported that the incorporation of EG improved thermal conductivity and influenced phase transition properties. The research indicated that the melting point of the composite material was affected by the presence of EG, which altered the thermal behavior of the eutectic salts [J. Lopez. et.al, 2010]

Furthermore, the specific surface area and porosity of EG can induce changes in the melting and crystallization behavior of the salts. The interaction between the salt molecules and the EG surface may require additional energy for the phase transition, resulting in increased melting peak temperatures.

The latent heats were measured as 74.078J/kg, 65.277J/kg, 56.414J/kg, and 47.55J/kg for 3%, 5%, 7% and 9% respectively. The reduction in latent heat capacity with the addition of expanded graphite (EG) is primarily due to the dilution effect, as EG occupies space in the composite without contributing to the phase change. EG's non-participatory nature in the phase transition process reduces the proportion of active PCM, lowering the overall latent heat capacity. Studies on capric-myristic acid/EG and paraffin wax/EG composites confirm this effect, highlighting that while EG enhances thermal conductivity, it diminishes latent heat storage [D. Zhou et.al, 2024 and Y. Li et.al, 2024]

3.6. Thermal Conductivity

Figure 7 depicts the effect of EG weight percentage on the thermal conductivity. The void structure of EG can be improved by allowing more nitrate salts absorbed per unit volume. Comparing the prepared samples to pure $\text{KNO}_3/\text{NaNO}_3$, the thermal conductivity increased by 13% (3% EG), 21% (5% EG), 23% (3%EG) and 25% (9%EG) compared with pure $\text{KNO}_3/\text{NaNO}_3$. EG is an allotropic form of carbon with free electron in the valence shell that improves thermal conductivity. Carbon in the form of allotropic was found in EG with a free electron in the valence shell, which improves thermal conductivity.

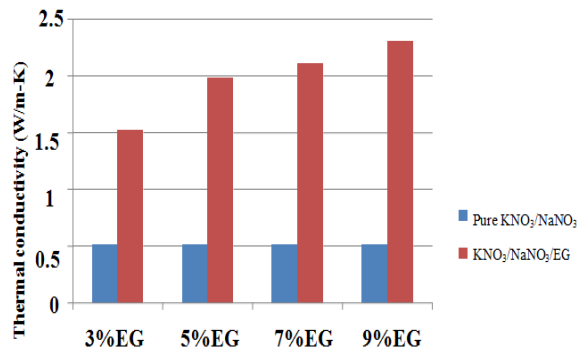


Figure7. Effect of EG weight percentage on the thermal conductivity

4. CONCLUSION

In the present work, new NEPCMs were prepared and characterized for microstructural, chemical and thermal properties.

- New composite materials were discovered to increase the efficiency of the system, namely PCM's incorporated with EG. Here PCM's found to be inorganic in nature. This composite is ideal for medium temperature an application which is ranging from 200 to 300 degrees Celsius.
- The SEM and EDX images are obtained by changing the scanning range of the electron beam at different magnifications. The results revealed that the microstructures of potassium nitrate and sodium nitrate differed significantly, with potassium nitrate having a layered structure and sodium nitrate having a network structure. Because of a structural difference, the performance and characteristics of the mixture differ.
- When the microstructure and chemical composition of KNO₃-NaNO₃/EG are compared, it is discovered that EG can physically and chemically integrate with molten salts. As a result, it is an effective method for improving the performance of molten salts, as the EG appears to be an efficient element for improving molten salt efficiency.
- Heterogeneous nucleation has proven to be effective without inducing any chemical interaction with the pure PCM, a conclusion drawn from the discernible XRD and FTIR characteristic peaks.
- By DSC analysis we found melting point increased with increase of the percentage of NPs, when it comes to latent heat it shows decreases with increase of the NPs.
- Thermal conductivity of the prepared NEPCMs is observed to be increased with increasing the weight percentage of expanded graphite.
- These effects were discovered as a result of intermolecular interactions, surface characteristics, and thermal properties of the prepared NPs, which all contributed to significant improvement of the NEPCMs.

Acknowledgement

The authors are grateful to the Department of Mechanical Engineering, Siddaganga institute of

Technology, Tumkuru, Karnataka, for the assistance provided to achieve this research.

REFERENCES

- [1] Lazaro, P. Dolado, J.M. Marin, B. Zalba, "PCM-air heat exchangers for free-cooling applications in buildings: Experimental results of two real-scale prototypes," *Energy Conversion and Management*, Vol. 50, 2009, pp. 439–443. <https://doi.org/10.1016/j.enconman.2008.10.020>.
- [2] A.A. Al-Abidi, S. Bin Mat, K. Sopian, M.Y. Sulaiman, C.H. Lim, A. Th, "Review of thermal energy storage for air conditioning systems," *Renewable and Sustainable Energy Reviews*, Vol. 16, No. 8, 2012, pp. 5802–5819. <https://doi.org/10.1016/j.rser.2012.05.030>.
- [3] K. Kant, A. Shukla, A. Sharma, "Ternary mixture of fatty acids as phase change materials for thermal energy storage applications," *Energy Reports*, Vol. 2, 2016, pp. 274–279. <https://doi.org/10.1016/j.egy.2016.01.004>.
- [4] L.M. Bal, S. Satya, S.N. Naik, V. Meda, "Review of solar dryers with latent heat storage systems for agricultural products," *Renewable and Sustainable Energy Reviews*, Vol. 15, No. 1, 2011, pp. 876–880. <https://doi.org/10.1016/j.rser.2010.09.015>.
- [5] L.M. Bal, S. Satya, S.N. Naik, "Solar dryer with thermal energy storage systems for drying agricultural food products: A review," *Renewable and Sustainable Energy Reviews*, Vol. 14, No. 8, 2010, pp. 2298–2314. <https://doi.org/10.1016/j.rser.2010.04.014>.
- [6] M.J. Huang, P.C. Eames, B. Norton, "Phase change materials for limiting temperature rise in building integrated photovoltaics," *Solar Energy*, Vol. 80, No. 9, 2006, pp. 1121–1130. <https://doi.org/10.1016/j.solener.2005.10.006>.
- [7] P.H. Biwole, P. Eclache, F. Kuznik, "Phase-change materials to improve solar panel's performance," *Energy and Buildings*, Vol. 62, 2013, pp. 59–67. <https://doi.org/10.1016/j.enbuild.2013.02.054>.
- [8] R. Pasupathy, R. Velraj, R.V. Seeniraj, "Phase change material-based building architecture for thermal management in residential and commercial establishments," *Renewable and Sustainable Energy Reviews*, Vol. 12, No. 1, 2008, pp. 39–64. <https://doi.org/10.1016/j.rser.2006.05.010>.
- [9] S.M. Shalaby, M.A. Bek, A.A. El-Sebaei, "Solar dryers with PCM as energy storage medium: A review," *Renewable and Sustainable Energy Reviews*, Vol. 33, 2014, pp. 110–116. <https://doi.org/10.1016/j.rser.2014.01.085>.
- [10] A Sharma, V.V. Tyagi, C.R. Chen, D. Buddhi, "Review on thermal energy storage with phase change materials and applications," *Renewable and Sustainable Energy Reviews*, Vol. 13, No. 2, 2009, pp. 318–345. <https://doi.org/10.1016/j.rser.2007.10.005>.
- [11] V.V. Tyagi, D. Buddhi, "PCM thermal storage in buildings: A state of art," *Renewable and Sustainable Energy Reviews*, Vol. 11, No. 6, 2007, pp. 1146–1166. <https://doi.org/10.1016/j.rser.2005.10.002>.
- [12] M. Waqas, Z. Ud Din, "Phase change material (PCM) storage for free cooling of buildings—A review," *Renewable and Sustainable Energy Reviews*, Vol. 18, 2013, pp. 607–625. <https://doi.org/10.1016/j.rser.2012.10.034>.
- [13] Yang, X., Li, Z., Wu, H., et al., "Solar salt doped with expanded graphite for concentrated solar power systems: Enhanced thermal conductivity and stability," *Energy Conversion and Management*, Vol. 175, 2018, pp. 87–95. <https://doi.org/10.1016/j.enconman.2018.09.023>.
- [14] Zhou, Y., Wang, J., Li, Q., et al., "Thermal performance of solar salt/expanded graphite composites during thermal cycling," *Renewable Energy*, Vol. 158, 2020, pp. 392–401. <https://doi.org/10.1016/j.renene.2020.06.019>.

- [15] Chen, Y., Liu, R., Zhang, F., "Enhanced thermal conductivity and latent heat storage of solar salt using expanded graphite and carbon nanotubes," *Applied Thermal Engineering*, Vol. 125, 2017, pp. 589–596. <https://doi.org/10.1016/j.applthermaleng.2017.07.001>
- [16] Li, T., Zhang, P., Wang, H., "Improvement of thermal stability in solar salt with 3 wt% expanded graphite over 300 thermal cycles," *Solar Energy Materials and Solar Cells*, Vol. 232, 2022, Article 111341. <https://doi.org/10.1016/j.solmat.2021.111341>.
- [17] Sun, L., Zhou, X., Zhang, X., "Development of composite PCM with 5 wt% expanded graphite: Improved thermal conductivity and thermal storage," *Energy Storage Materials*, Vol. 2, No. 1, 2016, pp. 78–85. <https://doi.org/10.1016/j.ensm.2016.04.001>.
- [18] Salem Nijmeh, Bashar Hammad, Mohammad Al-Abed, Riad Bani-Khalid, "A Technical and Economic Study of a Photovoltaic-Phase Change Material (PV-PCM) System in Jordan," *Jordan Journal of Mechanical and Industrial Engineering*, Vol. 14, No. 4, December 2020, ISSN 1995-6665, pp. 371–379. <https://jjmie.hu.edu.jo/vol14-4/02-119-20.pdf>
- [19] M. Al Zou'bi, "Renewable Energy Potential and Characteristics in Jordan," *Jordan Journal of Mechanical and Industrial Engineering*, Vol. 4, No. 1, January 2010, ISSN 1995-6665, pp. 45–48. <https://jjmie.hu.edu.jo/files/v4n1/7.pdf>
- [20] K. V. Gangadharan, K. S. Umashankar, Ravish, V. Desai, "Machining Characteristics of Multiwall-CNT Reinforced Al/Al-Si Composites using Recurrence Quantification Analysis," *Jordan Journal of Mechanical and Industrial Engineering*, Vol. 5, No. 4, August 2011, ISSN 1995-6665, pp. 345–351. <https://jjmie.hu.edu.jo/files/v5n4/6.pdf>
- [21] Malek Ali, Samer Falih, "Synthesis and Characterization of Aluminum Composites Materials Reinforced with TiC Nano-Particles," *Jordan Journal of Mechanical and Industrial Engineering*, Vol. 8, No. 5, October 2014, ISSN 1995-6665, pp. 257–264. <https://jjmie.hu.edu.jo/files/v8n5/1.pdf>
- [22] Maher M. Al-Maghalseh, "Investigate the Natural Convection Heat Transfer in A PCM Thermal Storage System Using ANSYS/FLUENT," *Jordan Journal of Mechanical and Industrial Engineering*, Vol. 11, No. 4, December 2017, ISSN 1995-6665, pp. 217–223. <https://jjmie.hu.edu.jo/files/v11n4/1.pdf>
- [23] Mohamad I. Al-Widyan, Borhan A. Albiss, Mohammad S. Ali, "Effect of Alkaline Nitrates and Operating Temperature on the Performance of Dye-Sensitized Solar Cells," *Jordan Journal of Mechanical and Industrial Engineering*, Vol. 15, No. 3, August 2021, ISSN 1995-6665, pp. 309–318. <https://jjmie.hu.edu.jo/files/v15n3/10.pdf>
- [24] Hassan Hadi Sadiq, Munther Abdullah Mussa, "Experimental Study of Thermal Conductivity Effect on the Performance of Thermal Energy Storage," *Jordan Journal of Mechanical and Industrial Engineering*, Vol. 16, No. 4, September 2022, ISSN 1995-6665, pp. 557–565. <https://jjmie.hu.edu.jo/files/v16n4/12.pdf>
- [25] J. Lopez, Z. Acem, E. P. Del Barrio, "KNO₃/NaNO₃-Graphite materials for thermal energy storage at high temperature: Part II.-Phase transition properties," *Applied Thermal Engineering*, Vol. 30, No. 11-12, 2010, pp. 1586–1593. <https://doi.org/10.1016/j.applthermaleng.2010.03.014>.
- [26] D. Zhou, S. Xiao, Y. Liu, "The Effect of Expanded Graphite Content on the Thermal Properties of Fatty Acid Composite Materials for Thermal Energy Storage," *Molecules*, Vol. 29, No. 13, 2024, pp. 3146. <https://doi.org/10.3390/molecules29133146>.
- [27] Y. Li, H. Yan, F. Yang, S. Li, C. Jiang, L. Xie, "Paraffin Wax-Expanded Graphite Composite Phase Change Materials with Enhancing Thermal Conductivity and Thermal Stability for Thermal Energy Storage," *Chemistry*, 23 December 2024. <https://doi.org/10.1002/slct.202404879>.